Properties of single-particle states in a fully self-consistent particle-vibration coupling approach

Li-Gang Cao,[1,2,3,4] G. Colò,[5,6] H. Sagawa,[7,8] and P. F. Bortignon[5,6]
[1]*Institute of Modern Physics, Chinese Academy of Science, Lanzhou 730000, China*
[2]*State Key Laboratory of Theoretical Physics, Institute of Theoretical Physics, Chinese Academy of Sciences, Beijing 100190, China*
[3]*Kavli Institute for Theoretical Physics China, CAS, Beijing 100190, China*
[4]*Center of Theoretical Nuclear Physics, National Laboratory of Heavy Ion Accelerator of Lanzhou, Lanzhou 730000, China*
[5]*Dipartimento di Fisica, Università degli Studi di Milano, via Celoria 16, 20133 Milano, Italy*
[6]*Istituto Nazionale di Fisica Nucleare (INFN), Sezione di Milano, via Celoria 16, 20133 Milano, Italy*
[7]*Center for Mathematics and Physics, University of Aizu, Aizu-Wakamatsu, Fukushima 965-8580, Japan*
[8]*RIKEN, Nishina Center, Wako 351-0198, Japan*
(Received 30 December 2013; published 14 April 2014)

The properties of single-particle states in the magic nuclei ^{40}Ca and ^{208}Pb, in particular the energies, spectroscopic factors, and the effective mass, have been studied in a fully self-consistent particle-vibration coupling (PVC) approach within the framework of Skyrme energy density functional theory. All selected phonons are obtained by the random phase approximation, and the same Skyrme interaction is also used in the PVC vertex. We focus on the effect of the noncentral two-body spin-orbit and tensor interactions on the single-particle properties. It has been found that the contributions of those terms are important to improve the results for ^{208}Pb. The calculated single-particle energies and spectroscopic factors are compared to available experimental data. The single-particle level density around the Fermi surface is significantly increased due to the effect of PVC.

DOI: 10.1103/PhysRevC.89.044314 PACS number(s): 21.10.Pc, 21.30.Fe, 21.60.Jz, 21.10.Jx

I. INTRODUCTION

Since the 1970s, the self-consistent mean field (SCMF) approaches have achieved great success in describing various properties of finite nuclei in their ground state, such as binding energies, root-mean-square radii, and deformations [1]. The SCMF approaches have been extended to describe the excited states, such as multipole giant resonances, and rotational bands of finite nuclei. In those approaches, one starts in general from an effective nucleon-nucleon interaction, such as a Skyrme or Gogny interaction or a relativistic Lagrangian, and the parameters of the effective interaction are fitted to the properties of nuclear matter and some selected data of finite nuclei. The total binding energy of a nucleus is expressed as the integral of the energy density that is, in turn, a function of the one-body densities; these are extracted from the single-particle wave functions that are, with their corresponding energies, obtained from the self-consistent solution of the Schrödinger or Dirac equations. In such calculations, the single-particle level density and the spectroscopic factors differ from the experimental findings mainly because of the following reason. In the mean field theory, the basic assumption is that particles move independently in the *static* average potential produced by the surrounding nucleons. Of course, this assumption is an ideal one. In practice, nucleons can make collisions with other nucleons or couple to the collective vibrations of the whole system. This is related to the concept of the so-called "dynamical effects" beyond the mean field approximation. To consider the fluctuations of the mean field potential, one must go beyond the mean field scheme, which means that the average potential is no longer static or energy independent, and is instead energy dependent.

For finite nuclei, the fluctuations of the average potential are usually described by an effective theory denoted the particle-vibration coupling (PVC) [2] model. It has been shown that the particle-vibration coupling affects strongly the energies of single-particle states around the Fermi surface and increases the single-particle level density [3–6]. In earlier times, the PVC calculations lacked any self-consistency since the Woods-Saxon potential was usually adopted to calculate the single-particle basis, and the interactions at the PVC vertex were chosen with a large degree of arbitrariness [3–10]. In a few cases, the Skyrme interaction was adopted both for the single-particle potential and PVC vertices, but using only the velocity-independent terms in the PVC vertices [11]. Recently, microscopic self-consistent PVC calculations have been performed within either the framework of the Skyrme energy density functionals [12–15] or the framework of relativistic (i.e., covariant) functionals [16,17].

So far, even when the central terms of the Skyrme force have been consistently included in the PVC vertex, the noncentral terms such as the two-body spin-orbit term or the tensor terms have been dropped in the calculations [12]. At the same time, recently much attention has been devoted to the tensor terms added to the Skyrme force with the goal to explain, e.g., the evolution of the single-particle levels in exotic nuclei [based on Hartree-Fock (HF) or Hartree-Fock-Bogoliubov (HFB) calculations] [18–27]. Moreover, within the HF plus self-consistent random phase approximation (RPA), some of us have investigated the effect of the tensor force on the multipole response of finite nuclei [28,29]. The response function of uniform matter, and the occurrence of possible instabilities, has been the subject of another recent study [30]. In the present work, we shall study the effect of the noncentral terms of the Skyrme interactions at the PVC vertex on the single-particle properties of finite nuclei. We will discuss the sensitivity of the energy shifts associated with the single-particle states, of the effective mass, and of the

spectroscopic factors, when the tensor interaction and the spin-orbit interaction are included in the PVC vertex. The calculations are performed for the double magic nuclei ^{40}Ca and ^{208}Pb. The Skyrme interactions adopted here are SLy5 [31] and T44 [21]. For the case of SLy5, the terms associated with the tensor force are simply added on top of the central force as in Ref. [19], whereas, in the case of T44, the tensor parameters are fitted on the same footing as the other Skyrme parameters. The ground states and the various excited states of the nuclei ^{40}Ca and ^{208}Pb are calculated on the basis of the fully self-consistent HF + RPA framework as in Ref. [32]. The coupling of the particles to the vibrations is derived from the same Skyrme force in a consistent way.

This paper is organized as follows. In Sec. II we will briefly report the main features of our Skyrme HF plus RPA and PVC models, as well as the definitions of other quantities which will be discussed later. The results are displayed, analyzed, and compared with available experimental data in Sec. III. Section IV is devoted to the summary and perspectives for future work(s).

II. METHOD

In this section, we will briefly report the theoretical method adopted in our calculations. More detailed information about the Skyrme HF plus RPA calculations can be found in Ref. [32]. First, we start by solving the Skyrme HF equations in the coordinate space: the radial mesh is 0.1 (0.15) fm for ^{40}Ca (^{208}Pb), and the maximum value of the radial coordinate is set to be 15 (24) fm for ^{40}Ca (^{208}Pb), respectively. In order to calculate unoccupied states at positive energy, the continuum has been discretized by adopting box boundary conditions. In this way, we obtain the energies as well as the wave functions for particle (p) and hole (h) states, which are the inputs for RPA calculations. We solve the RPA equations in the matrix formulation; all the hole states are considered when we build the particle-hole (p-h) configurations, while for the particle states we choose the lowest six (eight) unoccupied states for each value of l and j in the case, respectively, of ^{40}Ca (^{208}Pb). It has to be noted that, for ^{40}Ca, RPA produces instabilities if we include more than six shells when the tensor force is considered. For ^{40}Ca (^{208}Pb) we have considered natural parity phonons with multipolarity L ranging from 0 to 4 (from 0 to 5). For each multipole response we have checked that the RPA value of the energy-weighted sum rule exhausts almost 100% of the analytic value calculated from the double commutator.

After we obtain the RPA phonons, in our present PVC calculations only those having energy smaller than 30 MeV and fraction of the total isoscalar or isovector strength larger than 5% have been considered for the coupling with single-particle states. In Table I we present the properties of the low-lying states of ^{40}Ca and ^{208}Pb, which give important contributions to the PVC results (the available experimental data are also shown in Table I). The results are obtained by using the SLy5 and T44 parameter sets with and without consideration of the tensor force. We can see that the tensor force affects in a substantial way both the energies and the reduced transition probabilities of the low-lying states of ^{40}Ca and ^{208}Pb.

The energy of the single particle (s.p.) state i can be obtained by means of second-order perturbation theory. We use such an approach in the present work. The dressed single-particle energy ε_i is expressed as

$$\varepsilon_i = \varepsilon_i^{(0)} + \Delta\varepsilon_i, \tag{1}$$

where $\varepsilon_i^{(0)}$ is the single-particle energy given by mean field calculations and $\Delta\varepsilon_i$ is the energy shift calculated from the self-energy, that is,

$$\Delta\varepsilon_i = \Sigma_i\left(\omega = \varepsilon_i^{(0)}\right). \tag{2}$$

The self-energy Σ_i has the following expression:

$$\Sigma_i(\omega) = \frac{1}{2j_i+1}\left(\sum_{nL,p>F}\frac{|\langle i\|V\|p,nL\rangle|^2}{\omega-\varepsilon_p^{(0)}-\omega_{nL}+i\eta} + \sum_{nL,h<F}\frac{|\langle i\|V\|h,nL\rangle|^2}{\omega-\varepsilon_h^{(0)}+\omega_{nL}-i\eta}\right), \tag{3}$$

where $\varepsilon_p^{(0)}$ ($\varepsilon_h^{(0)}$) is the HF single-particle (hole) energy, and ω_{nL} is the energy of the phonon. The (small) imaginary part η is set to be 0.05 MeV in our calculations. The numerators contain the squared modulus of a reduced matrix element called PVC

TABLE I. Energies and reduced transition probabilities of the low-lying states in ^{40}Ca and ^{208}Pb obtained by HF+RPA with SLy5 and T44 parameter sets. The values in parentheses are the results obtained without the contribution of the tensor force. The experimental data are from Ref. [33].

	J^π	Theory				Experiment	
		SLy5		T44			
		Energy (MeV)	$B(EL,0\to L)$ (e^2 fm^{2L})	Energy (MeV)	$B(EL,0\to L)$ (e^2 fm^{2L})	Energy (MeV)	$B(EL,0\to L)$ (e^2 fm^{2L})
^{40}Ca	3^-	3.225(3.822)	$0.884(1.285)\times10^4$	1.366(1.508)	$0.852(1.280)\times10^4$	3.74	1.18×10^4
^{208}Pb	2^+	5.155(4.934)	$3.065(2.858)\times10^3$	4.549(5.105)	$2.478(2.785)\times10^3$	4.09	4.09×10^3
	3^-	3.585(3.671)	$4.928(6.374)\times10^5$	3.337(3.629)	$5.739(5.523)\times10^5$	2.61	6.21×10^5
	4^+	5.760(5.417)	$1.395(1.256)\times10^7$	4.655(5.684)	$0.782(1.382)\times10^7$	4.32	1.29×10^7
	5^-	4.022(4.560)	$2.881(4.898)\times10^8$	3.977(4.092)	$3.796(2.443)\times10^8$	3.19	4.62×10^8
		4.507(5.589)	$0.748(1.642)\times10^8$	4.532(5.021)	$0.345(1.929)\times10^8$	3.71	3.30×10^8

vertex, which is expressed as

$$\langle i\|V\|j,nL\rangle = \sqrt{2L+1}\sum_{ph} X^{nL}_{ph} V_L(ihjp) + (-)^{L+j_h-j_p} Y^{nL}_{ph} V_L(ipjh), \quad (4)$$

where V_L is the particle-hole coupled matrix element,

$$V_L(ihjp) = \sum_{\text{all } m}(-)^{j_j-m_j+j_h-m_h}\langle j_i m_i\, j_j - m_j|LM\rangle \times \langle j_p m_p\, j_h - m_h|LM\rangle\langle j_i m_i, j_h m_h|V|j_j m_j, j_p m_p\rangle. \quad (5)$$

Details of the derivation of Eq. (3) can be found in Ref. [12]. Our prescription for the model space in which the self-energy (3) is evaluated has been extensively used in the past. It is well known that if a zero-range force is employed the values of the self-energy diverge when the model space is enlarged. This problem has been solved so far in uniform matter through regularization techniques [34,35], whereas the first results concerning regularization in finite nuclei have been obtained only very recently [36].

The PVC effects are included in the energy-dependent self-energy Σ. In a uniform system, or in a finite system treated with the local density approximation, the single-particle energy can be written in a quite general fashion as

$$\varepsilon(k) = \frac{\hbar^2 k^2}{2m} + \Sigma(k,\varepsilon(k)). \quad (6)$$

Here the self-energy Σ includes both the HF potential and the dynamical contributions from PVC (or, eventually, further) correlations; we have emphasized that such self-energy is a function of the momentum k and energy ε. We can define an effective mass m^* through the relation

$$\frac{m^*}{m} = \frac{\hbar^2 k}{m}\left(\frac{d\varepsilon}{dk}\right)^{-1}. \quad (7)$$

The momentum dependence of Σ gives rise to a non-locality, or k mass $\widetilde{m}$ which is related to Σ by

$$\frac{\widetilde{m}}{m} = \left(1 + \frac{m}{\hbar^2 k}\frac{\partial\Sigma}{\partial k}\right)^{-1}. \quad (8)$$

The energy dependence of Σ leads, instead, to a so-called E mass or ω mass, $\overline{m}$, defined by

$$\frac{\overline{m}}{m} = \left(1 - \frac{\partial\Sigma}{\partial\varepsilon}\right). \quad (9)$$

Thus, the effective mass m^* can be expressed in term of $\widetilde{m}$ and $\overline{m}$,

$$\frac{m^*}{m} = \left(\frac{\widetilde{m}}{m}\right)_\alpha \times \left(\frac{\overline{m}}{m}\right)_\alpha. \quad (10)$$

Since we deal in this work with finite nuclei, we have stressed that these quantities are state dependent by labeling them with the quantum numbers α of the HF single-particle state.

In particular, for a HF state, the k mass $(\widetilde{m}/m)_\alpha$ can be written as

$$\left(\frac{\widetilde{m}}{m}\right)_\alpha = \int |\varphi_\alpha(r)|^2 \frac{\widetilde{m}(r)}{m} d^3r, \quad (11)$$

where $\widetilde{m}(r)$ is the effective mass associated with the given Skyrme set (which is density dependent and, therefore, radial dependent because of the nuclear density profile) while φ_α is the Skyrme HF wave function.

From the standard many-body theory, the energy-dependent self-energy enters the Dyson equation for the single-particle

TABLE II. The energies of the neutron single-particle states around the Fermi surface in ^{40}Ca calculated in various approximations. The spectroscopic factors obtained in the full calculation are also shown in this Table. The results are obtained by using SLy5 and T44 parameter sets. The experimental data are taken from Refs. [37,38].

		HF	PVC central		PVC central + S.O.		PVC full		$\varepsilon_i^{\text{exp}}$	Spectroscopic factors	
		$\varepsilon^{(0)}$	$\Delta\varepsilon_i$	ε_i	$\Delta\varepsilon_i$	ε_i	$\Delta\varepsilon_i$	ε_i		S_i^{th}	S_i^{exp}
SLy5	$1f_{5/2}$	−1.26	−1.36	−2.62	−1.07	−2.33	−2.11	−3.37	−1.56	0.849	0.95
	$2p_{1/2}$	−3.11	−1.95	−5.06	−1.54	−4.65	−2.04	−5.15	−4.20	0.778	0.70
	$2p_{3/2}$	−5.28	−1.88	−7.15	−2.44	−7.72	−2.98	−8.26	−5.84	0.823	0.91
	$1f_{7/2}$	−9.69	−0.83	−10.52	−1.30	−10.99	−1.56	−11.26	−8.36	0.893	0.77
	$1d_{3/2}$	−15.17	−0.62	−15.79	−0.54	−15.71	−1.67	−16.85	−15.64	0.886	0.94
	$2s_{1/2}$	−17.26	−1.13	−18.39	−1.51	−18.77	−2.12	−19.38	−18.19	0.845	0.82
	$1d_{5/2}$	−22.10	−0.31	−22.41	−0.65	−22.75	−1.07	−23.17	−22.39	0.923	0.90
T44	$1f_{5/2}$	−0.21	−2.00	−2.21	−2.59	−2.80	−2.67	−2.88	−1.56	0.696	0.95
	$2p_{1/2}$	−2.79	−2.68	−5.47	−3.43	−6.22	−4.15	−6.94	−4.20	0.773	0.70
	$2p_{3/2}$	−5.59	−2.78	−8.38	−3.97	−9.56	−4.25	−9.84	−5.84	0.676	0.91
	$1f_{7/2}$	−10.59	−1.10	−11.69	−1.66	−12.25	−1.89	−12.47	−8.36	0.815	0.77
	$1d_{3/2}$	−13.99	−1.16	−15.15	−2.92	−16.91	−3.32	−17.31	−15.64	0.737	0.94
	$2s_{1/2}$	−17.18	−1.51	−18.69	−3.85	−21.03	−4.14	−21.32	−18.19	0.746	0.82
	$1d_{5/2}$	−22.59	−0.49	−23.08	−0.78	−23.37	−0.74	−23.34	−22.39	0.772	0.90

Green's function G, namely

$$\left[\varepsilon - \varepsilon_\alpha^{(0)} - \Sigma_\alpha(\varepsilon)\right] G_\alpha(\varepsilon) = 1. \quad (12)$$

We work here in the so-called diagonal approximation, in which one neglects the nondiagonal matrix elements $\Sigma_{\alpha\beta}$ on the HF basis [3] and we label $\Sigma_{\alpha\alpha}$ simply by Σ_α. The poles of the Green's function $G_\alpha(\varepsilon)$ correspond to the zeros of

$$f(\varepsilon) = \varepsilon - \varepsilon_\alpha^{(0)} - \Sigma_\alpha(\varepsilon), \quad (13)$$

and for each value of α there are several poles $\varepsilon_\alpha^\lambda$ characterized by the index λ; in other words, because of the coupling to the collective vibrations, the single-particle state α becomes fragmented. In the vicinity of a given pole $\varepsilon_\alpha^\lambda$ the Green's function can be represented (leaving aside a small "background" part) as

$$G_\alpha^\lambda(\varepsilon) = \frac{S_\alpha^\lambda}{\varepsilon - \varepsilon_\alpha}, \quad (14)$$

where the residues at these poles correspond to the usual definition of spectroscopic factors S_α^λ, which is given by

$$S_\alpha^\lambda = \left(1 - \frac{\partial \Sigma_\alpha}{\partial \varepsilon}\right)^{-1}_{\varepsilon = \varepsilon_\alpha^\lambda}. \quad (15)$$

The above Eqs. (12)–(15) are quite general. In the current paper we stick, as already said, to perturbation theory, and the self-energy is calculated as in Eq. (3). Accordingly, the spectroscopic factors of the above Eq. (15) are also calculated only for the renormalized HF states, that is, $\varepsilon_\alpha^\lambda$ is restricted to be $\varepsilon_i^{(0)}$ of Eq. (1). Such spectroscopic factors are displayed in Table II. From the definition of S_α^λ, we can deduce the value of the energy-dependent effective mass $(\overline{m}/m)_\alpha$ by taking the inverse of the spectroscopic factor S_α^λ.

III. RESULTS AND DISCUSSION

In this section we shall present our results for two nuclei: ^{40}Ca and ^{208}Pb. The effective Skyrme interactions SLy5 and T44 are used in our calculations. We will stress, in our discussion, the effect of the non-central part of the Skyrme interaction (such as the spin-orbit and tensor terms) on the single-particle energies deduced from the PVC calculations.

A. Results for ^{40}Ca

In Fig. 1 and Table II we show the results for the energies ε_i of neutron single-particle levels around the Fermi surface in ^{40}Ca, calculated in various approximation. The symbols are the same as in Eqs. (1) and (15). The results (denoted by $\varepsilon^{(0)}$) in the third column are obtained within the HF mean field approximation by including the contribution of tensor interaction, although the tensor interaction gives almost no contribution to the single-particle energies in this case since ^{40}Ca is a $\vec{l}\cdot\vec{s}$ saturated nucleus (although we remind that it affects the energies and transition probabilities of the low-lying vibrations in ^{40}Ca [28]). The results in the fifth, seventh, and ninth columns in Table II correspond to the PVC calculations with the central Skyrme interaction, the central plus spin-orbit interaction, and the central plus spin-orbit as well as tensor interactions in the PVC vertex, respectively. The values in the columns labeled by $\Delta\varepsilon_i$ are the difference between the

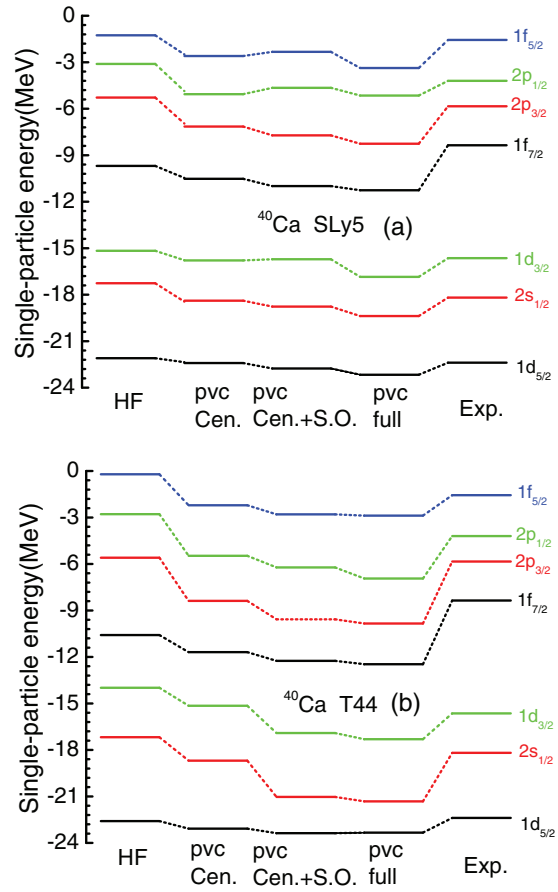

FIG. 1. (Color online) Neutron states in ^{40}Ca calculated with the parameter set SLy5 (upper panel) and T44 (lower panel). The various columns, from left to right, correspond to the HF calculation and to HF + PVC with only the central interaction in the vertex, to HF + PVC with central and spin-orbit interaction in the vertex, and to HF + PVC with central plus spin-orbit and tensor interactions in the vertex. The last column displays the experimental data.

PVC results and the original HF values. The results are also compared with the available experimental data.

The same information for the single-particle energies is shown in Fig. 1. From Table II and Fig. 1, we can see that the single-particle energies, both below and above the Fermi energy, become more negative when the calculation includes the PVC effects. This qualitative outcome has been already found and explained in Ref. [12]. For the PVC results obtained with only the central terms of the Skyrme force in the vertex, the maximum energy shift is -1.95 MeV (-2.78 MeV) for the $2p_{1/2}$ ($2p_{3/2}$) state using the SLy5 (T44) interaction. The spin-orbit interaction shows a repulsive effect on the energies of various giant resonances in light nuclei, and an attractive effect in heavy nuclei when included as a residual interaction in the RPA calculations. In the PVC calculations, from Table II we see that it gives a repulsive contribution to the energy shift for some states and an attractive contribution for some other states in the case of the SLy5 force, while if one moves to the T44 force, the spin-orbit interaction always gives an attractive contribution for all single-particle states. We will now discuss the contribution from tensor terms. From Table II, we can see that the tensor

TABLE III. The calculated effective mass around the Fermi surface for neutrons in ^{40}Ca in various approximations. The results are obtained by using the SLy5 and T44 parameter sets.

	HF	PVC central		PVC central + S.O.		PVC full	
	$\widetilde{m}/m$	$\overline{m}/m$	m^*/m	$\overline{m}/m$	m^*/m	$\overline{m}/m$	m^*/m
SLy5	0.852	1.091	0.931	1.107	0.944	1.170	0.999
T44	0.857	1.153	0.988	1.313	1.127	1.347	1.155

force gives an attractive contribution to the energy shift of all the single-particle levels, for both the SLy5 and T44 Skyrme forces. We have also calculated the r.m.s. deviation σ between theoretical and experimental single-particle states. The value of σ is 1.026 (1.578), 1.330 (1.975), 1.566 (2.755), and 2.393 (3.010) in the cases of HF, PVC with central terms, PVC plus central and spin-orbit terms, and full PVC calculation performed with SLy5 (T44), respectively. These results would go in the direction of calling for a refit of the Skyrme parameters.

In Table II, we also show the calculated spectroscopic factors of single-particle states and the corresponding experimental data. The results that we display are obtained by the full calculation (all terms in the PVC vertex). For the SLy5 parameter set, the calculated and measured values are more or less the same both for the particle and hole states. For the T44 parameter set the calculated results are systematically smaller than the experimental data for hole states. For the particle states, the results do not show a clear tendency.

In Table III we show the effective k mass, E mass, and the total effective mass in ^{40}Ca within various approximation. These are obtained by averaging the effective masses associated with the single-particle states that we have calculated (the averages being, of course, done with the proper weights $2j_\alpha + 1$). The effective k mass is about 0.85 around the Fermi surface within the pure Hartree-Fock mean field calculation for both the SLy5 and T44 parameter sets. When one goes beyond the mean field calculation, the mass operator is not only momentum dependent but also energy dependent: we can see that the calculated E mass is approximately in the range between 1.09 and 1.35 around the Fermi surface. The effective mass, which is the product of k mass and E mass, is $\approx$1. We conclude that the level density around the Fermi surface is enhanced when we go beyond the mean field approximation using the PVC model.

B. Results for ^{208}Pb

In Table IV we show the results for the energies ε_i of neutron single−particle levels around the Fermi surface in

TABLE IV. The same as Table II in the case of the nucleus ^{208}Pb. The experimental data are taken from Refs. [37,38].

		HF	PVC central		PVC central + S.O.		PVC full			Spectroscopic factors	
		$\varepsilon^{(0)}$	$\Delta\varepsilon_i$	ε_i	$\Delta\varepsilon_i$	ε_i	$\Delta\varepsilon_i$	ε_i	$\varepsilon_i^{\rm exp}$	S_i^{th}	$S_i^{\rm exp}$
SLy5	$3d_{3/2}$	0.335	−0.41	−0.07	−0.337	−0.002	−0.326	0.009	−1.40	0.911	1.09
	$2g_{7/2}$	0.15	−0.69	−0.54	−0.47	−0.32	−0.64	−0.49	−1.44	0.870	1.05
	$4s_{1/2}$	−0.10	−0.31	−0.41	−0.34	−0.44	−0.31	−0.41	−1.90	0.922	0.98
	$3d_{5/2}$	−0.65	−0.59	−1.24	−0.68	−1.33	−0.71	−1.36	−2.37	0.834	0.98
	$1j_{15/2}$	−1.20	−0.77	−1.97	−1.30	−2.50	−1.42	−2.62	−2.51	0.656	0.58
	$1i_{11/2}$	−1.02	−0.43	−1.45	−0.48	−1.50	−0.49	−1.51	−3.16	0.904	0.86
	$2g_{9/2}$	−3.22	−0.52	−3.74	−0.64	−3.86	−0.57	−3.79	−3.94	0.869	0.83
	$3p_{1/2}$	−8.05	−0.05	−8.10	0.01	−8.04	−0.18	−8.23	−7.37	0.889	0.90
	$2f_{5/2}$	−8.95	0.05	−8.90	0.16	−8.79	−0.01	−8.96	−7.94	0.883	0.60
	$3p_{3/2}$	−9.19	0.06	−9.13	0.05	−9.14	−0.16	−9.35	−8.26	0.858	0.88
	$1i_{13/2}$	−10.19	0.16	−10.03	0.07	−10.12	−0.06	−10.25	−9.24	0.908	0.91
	$2f_{7/2}$	−12.07	1.07	−11.00	1.33	−10.74	1.58	−10.49	−9.81	0.534	0.95
	$1h_{9/2}$	−12.07	0.21	−11.86	0.45	−11.62	0.45	−11.62	−11.40	0.789	0.98
T44	$3d_{3/2}$	0.20	−0.55	−0.35	−0.44	−0.24	−0.44	−0.24	−1.40	0.895	1.09
	$2g_{7/2}$	0.14	−0.85	−0.71	−0.53	−0.39	−0.61	−0.47	−1.44	0.832	1.05
	$4s_{1/2}$	−0.35	−0.48	−0.83	−0.50	−0.85	−0.47	−0.82	−1.90	0.896	0.98
	$3d_{5/2}$	−0.88	−0.72	−1.60	−0.81	−1.69	−0.81	−1.69	−2.37	0.855	0.98
	$1j_{15/2}$	−0.30	−0.87	−1.17	−1.80	−2.10	−1.77	−2.07	−2.51	0.583	0.58
	$1i_{11/2}$	−2.19	−0.39	−2.58	−0.51	−2.70	−0.57	−2.76	−3.16	0.884	0.86
	$2g_{9/2}$	−3.28	−0.52	−3.80	−0.69	−3.97	−0.68	−3.96	−3.94	0.877	0.83
	$3p_{1/2}$	−7.91	−0.08	−7.99	0.04	−7.87	0.03	−7.88	−7.37	0.905	0.90
	$2f_{5/2}$	−8.92	0.03	−8.89	0.19	−8.72	0.18	−8.74	−7.94	0.888	0.60
	$3p_{3/2}$	−9.14	0.11	−9.03	0.19	−8.95	0.21	−8.93	−8.26	0.844	0.88
	$1i_{13/2}$	−9.18	0.17	−9.01	−0.01	−9.19	0.01	−9.17	−9.24	0.903	0.91
	$2f_{7/2}$	−12.10	0.54	−11.56	0.49	−11.61	0.68	−11.42	−9.81	0.580	0.95
	$1h_{9/2}$	−13.14	0.13	−13.01	0.43	−12.71	0.44	−12.70	−11.40	0.831	0.98

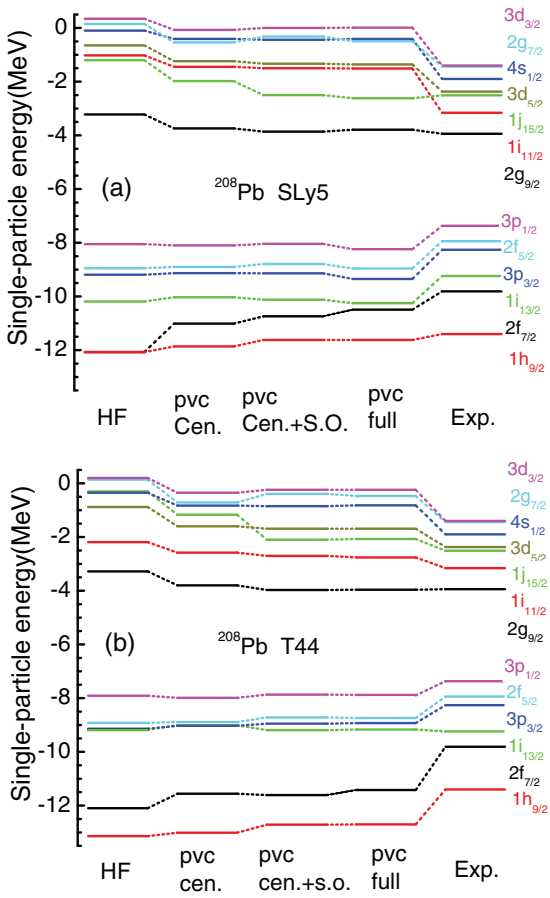

FIG. 2. (Color online) The same as Fig. 1 in the case of the nucleus ^{208}Pb.

^{208}Pb calculated within various approximations, exactly as in the case of ^{40}Ca that we have just discussed. The results given by the HF mean-field approximation, denoted by $\varepsilon^{(0)}$ in the third column, are obtained by including the contribution of the tensor interaction. There are finite contributions of the tensor terms to the single-particle energies in the ground state of ^{208}Pb which is not a $\vec{l}\cdot\vec{s}$ saturated nucleus. The results are compared with the available experimental data. The same theoretical and experimental energies are displayed in Fig. 2.

From Table IV and Fig. 2, we can see that the PVC calculations give a small repulsive contribution to the energy for most of the hole states below the Fermi surface. One noticeable exception is the $2f_{7/2}$ hole state which is shifted up in energy by about 1.60 MeV in the case of the SLy5 parameter set, and by 0.70 MeV in the case of the T44 parameter set. On the other hand, for its spin-orbit partner state $2f_{5/2}$ the energy shift is rather small. This goes against the prejudice that spin-orbit partner states should be affected more or less in the same way by the PVC effects: in this case, the special role of the coupling with the low-lying 3^- breaks this rule of thumb. For the particle states, the energy shift $\Delta\varepsilon_i$ is always negative but its magnitude depends on the state chosen and on the approximation scheme. In particular, the spin-orbit and tensor terms of the force do not give a systematic effect: for some states they give a repulsive contribution to the energy

TABLE V. The same as Table III in the case of the nucleus ^{208}Pb.

	HF	PVC central		PVC central + S.O.		PVC full	
	$\widetilde{m}/m$	$\overline{m}/m$	m^*/m	$\overline{m}/m$	m^*/m	$\overline{m}/m$	m^*/m
SLy5	0.839	1.156	0.968	1.198	1.002	1.229	1.028
T44	0.841	1.157	0.973	1.200	1.009	1.235	1.038

shift (with respect to the shift obtained by retaining only the central part of the Skyrme force at the PVC vertex), whereas for some other states they give attractive contributions. We have also calculated the r.m.s. deviation σ between theoretical and experimental single-particle states. The values of σ are 1.451, 1.030, 0.993, 1.097 for SLy5 and 1.421, 1.002, 0.907, 0.873 for T44 in the cases of HF, PVC with central terms, PVC with central plus spin-orbit terms, and full PVC calculations, respectively. In this case the inclusion of all terms in the PVC vertex produces an improvement of the results, although such improvement is small.

In Table IV we also show the calculated spectroscopic factors of the single-particle states and the corresponding experimental data. The calculations are performed within our full PVC model. For the particle states, the agreement between the calculated and the measured spectroscopic factors is generally satisfactory. For the hole states, the largest disagreement between theoretical and experimental data is found in the case of the $2f_{5/2}$ and $2f_{7/2}$ states. For the $2f_{5/2}$ state, we can see that it is rather fragmented from the experimental side, whereas the calculated fragmentation is rather small. For its spin-orbit partner state $2f_{7/2}$, the situation is opposite.

In Table V, we show the effective k mass, E mass, and total effective mass in ^{208}Pb. As in the previous case of ^{40}Ca, we have averaged the effective masses of the states that we have considered (above and below the Fermi surface). The effective k mass is about 0.84 around the Fermi surface in the pure HF calculation with the SLy5 and T44 parameter sets. When one goes beyond the mean field calculation, we see that the calculated E mass is approximately between 1.16 and 1.24 around the Fermi surface. The total effective mass, that is, the product of the k mass and E mass, of the states around the Fermi surface is about 1 (which is comparable to the empirical value).

IV. SUMMARY

In this paper, the properties of the single-particle states, in particular the energies, the spectroscopic factors, and the effective masses in the magic nuclei ^{40}Ca and ^{208}Pb have been studied in a fully self-consistent particle-vibration coupling (PVC) approach within the framework of Skyrme energy density functional theory. All the vibrations (phonons) are produced within a fully self-consistent random phase approximation (RPA) scheme. The SLy5 and T44 parameter sets are adopted; the tensor terms are added to the central terms without any refit in the case of the SLy5 parameter set.

We have paid a specific attention to the effect produced on the single-particle properties by the noncentral part of the Skyrme interaction. It has been found, in the case of the single-particle energies, that the contributions to their energy shifts induced by the tensor and spin-orbit terms are smaller than those coming from the central Skyrme terms. In the case of the spin-orbit terms, the contribution to the single-particle energy shift is quite random for both ^{40}Ca and ^{208}Pb, namely it can be either positive or negative. The contribution to the energy shifts stemming from the tensor force is negative in ^{40}Ca, while it has a random sign for ^{208}Pb.

For ^{208}Pb using the set T44, our results are improved with respect to the experimental findings by the contributions of spin-orbit and tensor forces. The calculated single-particle energies and spectroscopic factors show an overall good agreement with data. This is reflected in the enhancement of the single-particle level density around the Fermi surface, due to the PVC correlations. The effective mass becomes indeed close to 1 around the Fermi energy, and this is consistent with the empirical information.

This work is a further step in the direction of improving mean-field models when they need to be compared with the single-particle states and their fragmentation. The role of higher-order processes, beyond our simple perturbation theory approach, should be investigated. More importantly, we should see if more significant improvements in the agreement between theory and experiment can be obtained when the effective force is refitted.

The coupling between single-particle and collective degrees of freedom is also important if one wants to describe of the optical potential that characterized finite nuclei when projectile nucleons interact in, e.g., a scattering process. The particle-vibration coupling can provide an important contribution to the imaginary part of the optical potential. Work in this direction is also in progress.

ACKNOWLEDGMENTS

L.G.C. acknowledges the support of the National Science Foundation of China under Grants No. 10875150 and No. 11175216, and the Project of Knowledge Innovation Program of Chinese Academy of Sciences under Grant No. KJCX2-EW-N01. This work is partially supported by the Japanese Ministry of Education, Culture, Sports, Science and Technology by a Grant-in-Aid for Scientific Research under Program No. (C(2))20540277. The support of the Italian Research Project "Many-body theory of nuclear systems and implications on the physics of neutron stars" (PRIN 2008) is also acknowledged.

[1] M. Bender, P.-H. Heenen, and P.-G. Reinhard, Rev. Mod. Phys. **75**, 121 (2003).
[2] A. Bohr and B. R. Mottelson, *Nuclear Structure*, Vol. II (W. A. Benjamin, New York, 1975).
[3] P. Ring and E. Werner, Nucl. Phys. A **211**, 198 (1973).
[4] I. Hamamoto and P. Siemens, Nucl. Phys. A **269**, 199 (1976).
[5] P. F. Bortignon, R. A. Broglia, C. H. Dasso, and C. Mahaux, Phys. Lett. B **140**, 163 (1984).
[6] C. Mahaux, P. F. Bortignon, R. A. Broglia, and C. H. Dasso, Phys. Rep. **120**, 1 (1985).
[7] G. F. Bertsch and T. T. S. Kuo, Nucl. Phys. A **112**, 204 (1968).
[8] J. Wambach, V. K. Mishra, and L. Chu-Hsia, Nucl. Phys. A **380**, 285 (1982).
[9] H. M. Sommermann, K. F. Ratcliff, and T. T. S. Kuo, Nucl. Phys. A **406**, 109 (1983).
[10] R. P. J. Perazzo, S. L. Reich, and H. M. Sofia, Nucl. Phys. A **339**, 23 (1980).
[11] V. Bernard and N. V. Giai, Nucl. Phys. A **348**, 75 (1980).
[12] G. Colò, H. Sagawa, and P. F. Bortignon, Phys. Rev. C **82**, 064307 (2010).
[13] K. Mizuyama, G. Colò, and E. Vigezzi, Phys. Rev. C **86**, 034318 (2012).
[14] M. Brenna, G. Colò, and P. F. Bortignon, Phys. Rev. C **85**, 014305 (2012).
[15] K. Mizuyama and K. Ogata, Phys. Rev. C **86**, 041603 (2012).
[16] E. Litvinova and P. Ring, Phys. Rev. C **73**, 044328 (2006).
[17] E. V. Litvinova and A. V. Afanasjev, Phys. Rev. C **84**, 014305 (2011).
[18] B. A. Brown, T. Duguet, T. Otsuka, D. Abe, and T. Suzuki, Phys. Rev. C **74**, 061303(R) (2006).
[19] G. Colò, H. Sagawa, S. Fracasso, and P. F. Bortignon, Phys. Lett. B **646**, 227 (2007); see also **668**, 457 (2008).
[20] D. M. Brink and F. Stancu, Phys. Rev. C **75**, 064311 (2007).
[21] T. Lesinski, M. Bender, K. Bennaceur, T. Duguet, and J. Meyer, Phys. Rev. C **76**, 014312 (2007).
[22] M. Grasso, Z. Y. Ma, E. Khan, J. Margueron, and N. Van Giai, Phys. Rev. C **76**, 044319 (2007).
[23] M. Zalewski, J. Dobaczewski, W. Satula, and T. R. Werner, Phys. Rev. C **77**, 024316 (2008).
[24] T. Otsuka, T. Suzuki, R. Fujimoto, H. Grawe, and Y. Akaishi, Phys. Rev. Lett. **95**, 232502 (2005); T. Otsuka, T. Matsuo, and D. Abe, *ibid.* **97**, 162501 (2006).
[25] Y. Z. Wang, J. Z. Gu, X. Z. Zhang *et al.*, Phys. Rev. C **84**, 044333 (2011).
[26] J. M. Dong, W. Zuo, X. Z. Zhang *et al.*, Phys. Rev. C **84**, 014303 (2011).
[27] H. Sagawa and G. Colò, Prog. Part. Nucl. Phys. **76**, 76 (2014).
[28] L. G. Cao, H. Sagawa, and G. Colò, Phys. Rev. C **83**, 034324 (2011); **81**, 044302 (2010); L. G. Cao, G. Colo, H. Sagawa, P. F. Bortignon, and L. Sciacchitano, *ibid.* **80**, 064304 (2009).
[29] C. L. Bai, H. Q. Zhang, H. Sagawa, X. Z. Zhang, G. Colo, and F. R. Xu, Phys. Rev. C **83**, 054316 (2011); Phys. Rev. Lett. **105**, 072501 (2010).
[30] A. Pastore, M. Martini, V. Buridon, D. Davesne, K. Bennaceur, and J. Meyer, Phys. Rev. C **86**, 044308 (2012); A. Pastore, D. Davesne, Y. Lallouet, M. Martini, K. Bennaceur, and J. Meyer, *ibid.* **85**, 054317 (2012); D. Davesne, M. Martini, K.

Bennaceur, and J. Meyer, *ibid.* **80**, 024314 (2009); **84**, 059904 (2011).
[31] E. Chabanat, P. Bonche, P. Haensel, J. Meyer, and R. Schaeffer, Nucl. Phys. A **635**, 231 (1998).
[32] G. Colò, L. G. Cao, N. Van Giai, and L. Capelli, Comput. Phys. Commun. **184**, 142 (2013).
[33] http://www.nndc.bnl.gov.
[34] K. Moghrabi, M. Grasso, G. Colò, and N. Van Giai, Phys. Rev. Lett. **105**, 262501 (2010).
[35] K. Moghrabi, M. Grasso, X. Roca-Maza, and G. Colò, Phys. Rev. C **85**, 044323 (2012).
[36] M. Brenna *et al.* (unpublished).
[37] N. Schwierz, I. Wiedenhöver, and A. Volya, arXiv:0709.3525.
[38] A. Oros, Ph.D. thesis, University of Köln, 1996 (unpublished).